Analysis of photoentrainment in the diurnal zebrafish suggests a profound divergence with nocturnal rodents

Clair Chaigne[1], Dora Sapède[1,2] Xavier Cousin[3], Laurent Sanchou[4], Patrick Blader[1,5] and Elise Cau[1,5*]

[1] Unité de Biologie Moléculaire, Cellulaire et du Développement (MCD, UMR5077) Centre de Biologie Intégrative (CBI, FR 3743), Université de Toulouse 3/UPS, CNRS, UPS, France

[2] IRMB, Université de Montpellier, INSERM, Montpellier, France.
[3] MARBEC, Université de Montpellier, CNRS, Ifremer, IRD, INRAE, Route de Maguelone, F-34250 Palavas, France.
[4] Centre de Biologie Intégrative (CBI, FR 3743), Université de Toulouse 3/UPS, CNRS, UPS, France

[5] Equal contribution

[*]Corresponding author: elise.cau@univ-tlse3.fr

Classification: Biological Sciences. Neurosciences.

Contributions: CC: performed research, analyzed data, wrote the paper. DS, XC, LS, PB: contributed new reagents/analytic tools, EC: designed research, performed research, analyzed data, wrote the paper, contributed new reagents/analytic tools.

Abstract: The eye is instrumental for controlling circadian rhythms in nocturnal mammals. Here, we address the conservation of this function in the zebrafish, a diurnal vertebrate. Using *lakritz (lak)* mutant larvae, which lack retinal ganglion cells (RGCs), we show that while a functional eye is required for a phenomenon known as masking, it is largely dispensable for the establishment of circadian rhythms of locomotor activity. Furthermore, the eye is dispensable for the induction of a phase delay following a pulse of white light at CT 16 but contributes to the induction of a phase advance upon a pulse of white light at CT21. Melanopsin photopigments are important mediators of photoentrainment in nocturnal mammals. One of the zebrafish melanopsin genes, *opn4xa*, is expressed in RGCs but also in photosensitive projection neurons in the pineal gland. To address the role of this photopigment, we generated an *opn4xa* mutant. Abrogating *opn4xa* has no effect on masking and circadian rhythms of locomotor activity, or for the induction of phase shifts, but is required for period length control when larvae are subjected to constant light. Finally, analysis of *opn4xa;lak* double mutant larvae did not reveal redundancy between the function of the eye and Opn4xa in the pineal for photoentrainment or phase shifts after light pulses. Our results challenge the dogma that the eye as the sole mediator of light influences on circadian rhythms and highlight profound differences in the circadian system and photoentrainment between different animal models.

Significance statement: The eye in general and melanopsin expressing cells in particular are crucial for circadian rhythms in nocturnal mammals, most notably during photoentrainment, by which circadian rhythms adapt to a changing light environment. In marked contrast to this, we show that in the diurnal zebrafish the eye and photosensitivity dependent on the melanopsin gene *opn4xa,* which expressed in both the eye and the pineal gland, are largely dispensable for correct circadian rhythms. These results provide the first insight that the light sensors orchestrating circadian rhythms are different between animal models raising the intriguing possibility that vertebrates might employ different molecular/cellular circuits for photoentrainment depending on their phylogeny and/or temporal niche.

INTRODUCTION

Light has a profound influence on the physiology and behaviour of living organisms. In particular, it controls circadian rhythms that in turn regulate a phenomenal variety of biological functions. Circadian rhythms are defined by their period of approximately 24 hours. Once established, these rhythms persist in constant light conditions, which has fostered the concept of an endogenous time-keeping mechanism known as the circadian system. Nonetheless, external cues are required to synchronize (or 'entrain') circadian rhythms with the exogenous environmental conditions. For instance, light entrains the circadian system through a process referred to as photoentrainment (see (Bhadra et al., 2017) for a review).

In nocturnal mammals, photoentrainment depends on a functional retina. Enucleated mice or mice lacking retinal ganglion cells (RGCs) do not entrain to LD (Light/Dark) cycles and thus behave as if they were in constant darkness (Brzezinski et al., 2005; Freedman et al., 1999; Wee et al., 2002). More precisely, photoentrainment depends on a specific subtype of RGCs expressing the photopigment melanopsin, which is encoded by the *Opn4* gene. These RGCs are sensitive to blue light and are referred to as ipRGCs for "intrinsically photosensitive RGCs". Mice mutant for *Opn4* show a diminished phase-delay in response to a pulse of light administered at circadian time 16 (CT 16; at the beginning of the subjective night) but entrain normally to LD cycles (Panda et al., 2002; Ruby et al., 2002)**.** In contrast, mice with no ipRGCs or with impaired neurotransmission from ipRGCs show no entrainment to LD as well as no phase delay following a light pulse at CT16 (Güler et al., 2008; Kofuji et al., 2016). The difference between the phenotypes observed when only melanopsin photosensitivity is impaired compared to the models where ipRGCs inputs to the brain are lost is thought to result from the influence of classical rods and cone photoreceptors on ipRGCs. Indeed, both rods and cones have been shown to play a role during photoentrainment and to signal to ipRGCs (Altimus et al., 2008; Belenky et al., 2003; Calligaro et al., 2019; Dkhissi-Benyahya et al., 2007; Dollet et al., 2010; Perez-Leon et al., 2006; Wong et al., 2007). Thus, ipRGCs function as a hub that integrates and transmits photic information to the brain through a direct projection to the core of the suprachiasmatic nucleus (SCN; (Baver et al., 2008; Fernandez et al., 2016; Li and Schmidt, 2018)), which is thought to behave as a 'master clock' that synchronizes peripheral clocks present everywhere in the body. However, several other brain areas are capable of generating circadian oscillations when placed in culture (see (Dibner et al., 2010) for a review).

In addition to photoentrainment, ipRGCs also control the increase of period length when animals are placed in constant light (LL) (Panda et al., 2002; Ruby et al., 2002) and are required for a process of maturation of the circadian clock that sets the definitive period of locomotor rhythms in LD and DD (Chew et al., 2017). Finally, in addition to their crucial influence on the circadian system, murine ipRGCs also control masking, a direct suppressive effect of light on locomotor activity. This activity is thought to involve different ipRGC subtypes than the ones that impact the circadian system (Rupp et al., 2019). Although ipRGCs mediate circadian and direct effects of light on behaviour in nocturnal mammals, it is unclear if these roles are conserved in diurnal and non-mammalian species.

While the zebrafish has emerged as a powerful non-mammalian diurnal vertebrate model for chronobiology, the organization of the zebrafish circadian system is thought to differ from the mammalian one. First, the pineal gland is capable of driving autonomous rhythms of melatonin production when placed in culture owing to its intrinsic photosensitivity (Cahill, 1996) whereas the generation of such rhythms require the retina in mammals (see (Bailes and Lucas, 2010) for a review). Secondly, zebrafish larvae lacking the ventral diencephalon (including the putative SCN) exhibit normal circadian rhythms of gene expression in the pineal (Noche et al., 2011). Thirdly, all zebrafish adult organs tested, including the pineal gland, are directly photo-entrainable when placed in culture (see (Vatine et al., 2011) for a review). Further complexity arises from the large number of opsin genes in

the zebrafish genome (42 in total), including 5 melanopsin genes (Davies et al., 2015). All zebrafish melanopsin genes are expressed in the retina, including *opn4xa* and *opn4b* in larval RGCs (Kölsch et al., 2021; Matos-Cruz et al., 2011). In addition, melanopsin expression is detected in extra-retinal tissues. For instance, *opn4xa* is expressed in a subpopulation of projection neurons in the pineal gland (Sapède et al., 2020). Thus, while both ipRGCs and *opn4xa*+ pineal cells have been described in the zebrafish larvae, the roles of these cells are currently unknown.

To begin to address differences in the control of circadian rhythms between nocturnal mammals and zebrafish, we first analysed the function of the retina using *lakritz* (*lak*) mutants in which all RGCs fail to develop and as such no connection exist between the eye and the CNS (Kay et al., 2001). *lak* mutant larvae entrain to LD cycles and maintain rhythms of locomotor activity with a period similar to their control siblings in constant darkness (DD) but show subtle alterations in constant light (LL). While we detected no defect in phase shifting in response to a pulse of white light produced in the early subjective night (CT16) in *lak* -/- larvae, we observed a reduction of the phase shift induced upon a similar pulse of light at CT21 in *lak* mutants. To test the function of the intrinsic photosensitivity of ipRGCs and ipRGCs-like-cells of the pineal gland, we engineered an *opn4xa* mutant. *opn4xa* -/- larvae successfully entrain to LD cycles and maintain rhythms of locomotor activity in constant conditions albeit with a reduction of period in LL. Pulses of white light at CT16 and CT21 induced similar phase shifts in *opn4xa* mutant and *opn4xa*/*lak* double mutant larvae compared to controls. Our results suggest that the function of the retina and/or the intrinsic photosensitivity of ipRGCs-like-cells of the pineal gland are not absolutely required for circadian photoentrainment in zebrafish, thus further highlighting differences in the circadian system and circadian photoentrainment between nocturnal mammals and zebrafish.

RESULTS

The zebrafish eye is required for masking but dispensable for the establishment of circadian rhythms

Photoentrainment in nocturnal mammals requires a functional eye. We took advantage of *lak* mutant larvae that lack RGCs to address whether this role for the eye is conserved in the diurnal zebrafish. Homozygous *lak* mutant larvae lack neuronal connections between the eye and the brain and do not display an optomotor response (Covello et al., 2020; Kay et al., 2001; Neuhauss et al., 1999). In cycles of 14h light:10h dark (hereafter referred to as LD), both control and *lak* mutant larvae exhibit rhythms of locomotor activity that are aligned with the LD cycles (Fig 1B). However, compared to control larvae, *lak* mutant larvae show a specific reduction of activity during the day (Fig 1.B, supplemental Table 1). Control and *lak* mutant LD-entrained larvae placed in constant darkness (DD) demonstrate rhythms of locomotor activity with similar levels (Fig 1.C, supplemental Tables 2). In addition, the periods and amplitudes of the rhythms observed in DD did not significantly differ between the two backgrounds (Fig 1D, E). The reduction in activity observed during the day in LD conditions thus most likely reflects a masking problem in *lak* mutants rather than a defect in circadian control.

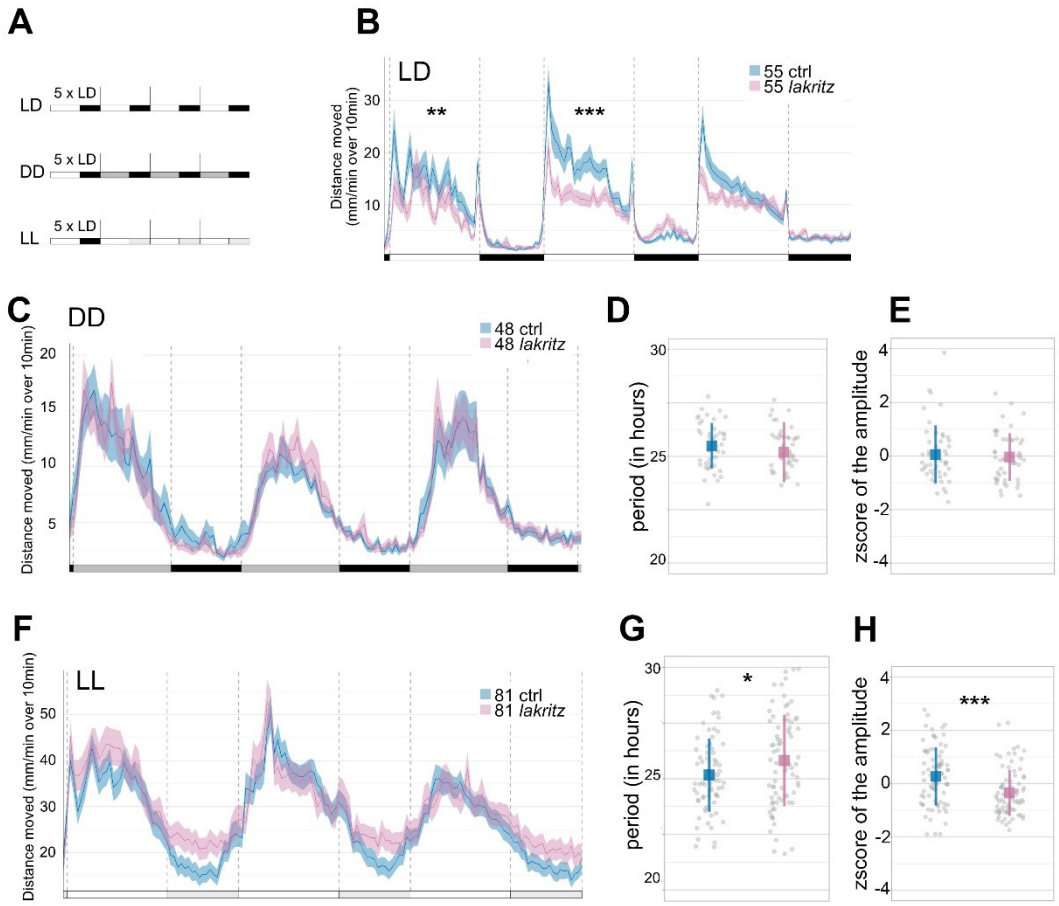

Figure 1: Locomotor activity of larvae devoid of RGCs in LD, DD and LL

A) Experimental design of LD, DD and LL experiments. White rectangles represent the day period, while black rectangles represent the night period, light grey rectangles represent the subjective day period and dark grey rectangles the subjective night. For each experiment, larvae are entrained for 5 LD cycles and their locomotor activity is tracked either in LD (LD), constant darkness (DD) or constant light (LL).

B) Average distance moved (mm/min over 10min) of 3 independent experiments in LD. Error bars represent SE. The distance moved is lower in *lak* larvae than control larvae during the 1st (p=0.008) and 2nd days (p=0.005) but not during the 3rd day (p=0.13) nor during the night (p=0.42, p=0.51 and p=0.57 for the 1st, 2nd and 3rd nights; Mann-Whitney two-tailed test), see supplementary Table 1.

C) Average distance moved (mm/min over 10min) of 2 independent experiments in DD (n=48 for control and *lak* larvae). Error bars represent SE. No differences are detected between the distance moved of control versus *lak* larvae using a Mann-Whitney two-tailed test for each subjective night or day, see supplementary Table 2.

D) Estimation of the periods using the FFT-NLLS method. Calculations were made on four complete cycles in DD. The mean period is not significantly different between control and *lak* larvae in DD (control: 25.48 ± 1.06 hours (n=48), *lak*: 25.18 ± 1.40 hours (n=48); mean ± S.D; p=0.31; Mann-Whitney two-tailed test, control vs *lak* larvae). Each grey point represents a single larva.

E) Z-score of the amplitude of circadian rhythm in control and *lak* larvae in DD. Estimation of the amplitude was generated using the FFT-NLLS method on four complete cycles in DD. Since we observed

differences in the overall amplitude of circadian rhythms between experiments in particular in LL, we calculated a zscore. Each grey point represents a single larva. No statistical difference between control and *lak* was observed.

F) Average distance moved (mm/min over 10min) of 3 independent experiments in LL (n=81 for control and *lak* larvae). Error bars represent SE. While the graph suggests a higher level of activity in *lak* larvae during the subjective night, the distance moved is not different between control and *lak* larvae for any subjective day or night (Mann-Whitney two-tailed test, see supplementary Table 3). In contrast, the amplitude is significantly reduced in *lak* compared to control larvae (see H).

G) Estimation of the periods using the FFT-NLLS method. Calculations were made on three complete cycles in LL. The mean period is significantly different between control and *lak* larvae in LL. Mean± sd (in hours) is represented. Each grey point represents a larva.

H) Z-score of the amplitude of circadian rhythm in control and *lak* larvae in three LL cycles. Estimation of the amplitude was generated using the FFT-NLLS method on the three independent experiments. Each grey point represents a single larva. *lak* larvae show a statistically reduced amplitude compared to controls ($p=9{,}47.10^{-5}$ using a T-test).

We next compared the activity of control and *lak* mutant LD-entrained larvae that are placed in constant light (LL) conditions. In two out of three experiments, we observed a reduced amplitude of circadian rhythms that leads to a statistically significant effect on the average of the three experiments (Figure 1 F, H). Furthermore, using the FFT-NLLS algorithm from the biodare web site (biodare2.ed.ac.uk), we observed a statistically significant effect on the period in LL, which is increased in *lak* mutant larvae (control: 25.16 ± 1.64 n=75, *lak*: 25.86 ± 2.10, n=81, p=0.041). In contrast, this effect was not significant when we used the mFourfit algorithm (control: 25.25 ± 1.911; *lak*: 25.67 ± 1.89 n=81 for both populations, p=0.13 using a Mann-Whitney two-tailed test) suggesting that the impact of the *lak* mutation on period in LL is subtle.

Altogether these results suggest that retinal ganglion cells and therefore a neuronal connection between the eye and the brain are dispensable for the establishment of circadian rhythms, their correct alignment to LD cycles and their maintenance in free running conditions (DD or LL) but required for the control of amplitude of locomotor activity in LL but not in DD.

Retinal Ganglion Cells are differentially required in a phase delay and a phase-advance paradigm of photoentrainment

To test for a role for RGCs in circadian photoentrainment, we assessed the phase-shifting effect of a pulse of white light on locomotor activity in *lak* larvae during the subjective night. We first chose to perform such a light pulse at CT16, as this was previously shown to induce a robust phase shift of the molecular clock in cell cultures (Tamai et al., 2007; Vallone et al., 2004). After entraining for 5 LD cycles, larvae from *lak+/-* incrosses were further reared in DD and subjected to a pulse of light during the second night in DD ("PD larvae"). Their activity was compared to the activity of larvae kept in the dark for 4 days ("DD larvae"). To analyze if a phase shift was induced, we calculated the difference of phase between the two last days ("after the light pulse") and the two first days ("before the light pulse"), a value we refer to as "△phase" (Fig 2.A). We found that a 2-hours pulse of light at CT16 induced a phase delay of locomotor activity rhythms in larvae, as the △phase of PD larvae was higher than the one of DD larvae (Fig 2.B, Table 1). When the difference between the Δphase of pulsed larvae minus the Δphase of larvae placed in DD was calculated, it suggests a phase delay of 2.5 hours on average in PD larvae. Finally, we determined that control and *lak* mutant larvae exhibit a similar phase shift in locomotor activity (Fig 2.C, Table 1) suggesting that RGCs are not necessary for the circadian

photoentrainment of locomotor activity to a pulse of light at the beginning of the subjective night (CT16).

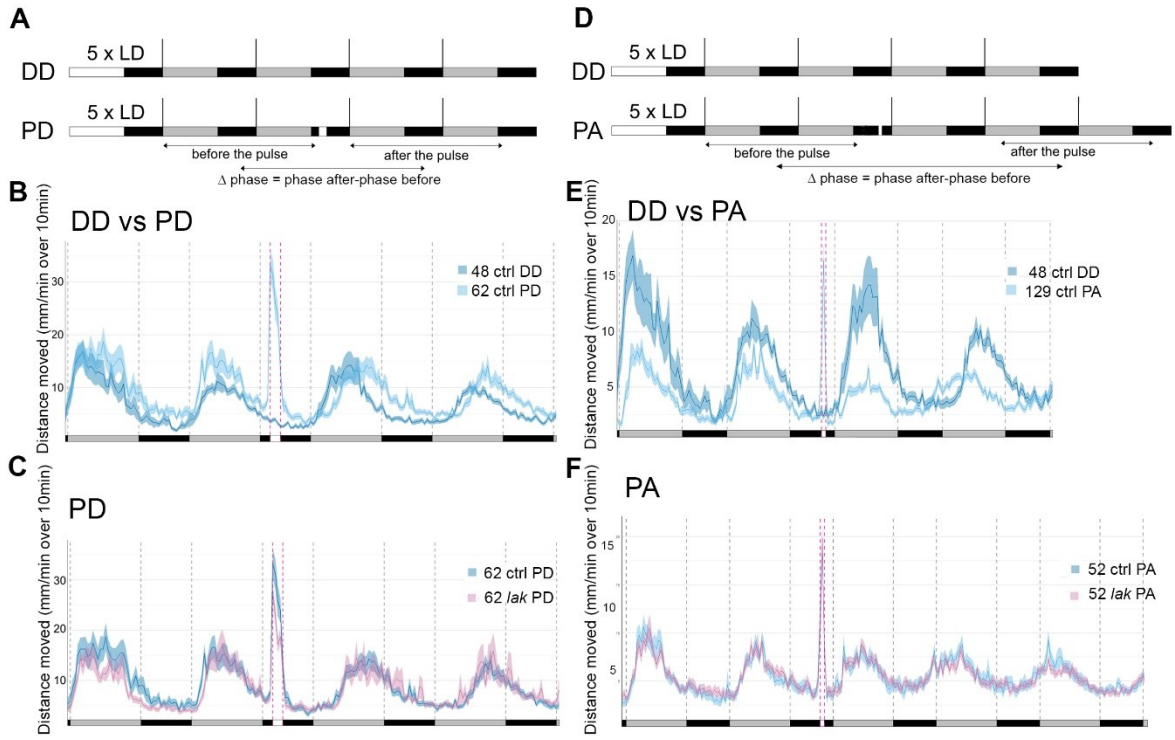

Figure 2: Larvae devoid of RGCs still photoentrain to pulses of white light at CT16 and CT21

A) Experimental design of phase delay (PD) experiments. White rectangles represent the day or light pulse period, black rectangles represent the night period and dark grey rectangles represent the subjective day. For each experiment, larvae are entrained for 5 LD cycles and their locomotor activity is tracked either in constant darkness for 4 days (DD) or tracked in constant darkness for 4 days and subjected to a 2-hours pulse of light during the night of the 2nd day of constant darkness at CT16 (PD). The phase of locomotor activity is calculated for each larva before and after the timing of the pulse for DD and PD experiments and the △phase (phase after the pulse – phase before the pulse) is calculated.
B) Average distance moved of control larvae (mm/min over 10min) in 2 independent DD experiments and 3 independent PD experiments. Mean ± SE. The △phase calculated using the FFT-NLLS method of PD larvae is higher than the one of DD larvae ($p<0.0001$, Mann-Whitney two-tailed test), showing that the pulse of light induced a phase delay.

C) Average distance moved (mm/min over 10min) of 3 independent PD experiments. Mean ± SE. The △phase of control versus *lak* larvae calculated using the FFT-NLLS method is not significantly different ($p=0.24$, Mann-Whitney two-tailed test). *lak* show lower levels of activity during the light pulse ($p=0.03$, Mann-Whitney two-tailed test).

D) Experimental design of phase advance (PA) experiments. The iconography is similar to A). After 5 training cycles in LD, PA-pulsed larvae were subjected to a one-hour pulse of light at CT21.

E) Average distance moved of control larvae (mm/min over 10min) in 2 independent DD experiments and 3 independent PA experiments. Mean ± SE. The △phase calculated using the FFT-NLLS method is negative in PA-pulsed larvae and statistically different from DD larvae (p<0.0001, Mann-Whitney two-tailed test), showing that the pulse of light induced a phase advance.

F) Average distance moved (mm/min over 10min) of 3 independent PA experiments. Mean ± SE.

We next performed a pulse of light at the end of the subjective night. A pulse of two hours of white light at CT21 induced a strong reduction of circadian amplitude making it difficult to assess a potential phase shift (Supplemental figure 1). In contrast, a one hour pulse induced a phase advance that could be detected during the second circadian cycle after the pulse (Figure 2D, E). Since this phase shift is not seen during the first cycle, we analyzed larvae over an additional cycle in order to obtain enough data to perform a robust phase calculation. The difference between the Δphase of pulsed larvae (PA) minus the Δphase of larvae placed in DD alone suggests that this paradigm induced a phase advance of at least 4.95 (2.61+2.34) hours on average. While *lak* -/- larvae showed a phase advance upon a pulse of light at CT21 (Fig 2.F, table1), this phase shift is weaker than that induced in control larvae (Δphase= -2.61 ± 4.05 for controls versus Δphase = -0.57 ± 4.1 for *lak* -/- larvae). These results suggest that a phase advance can occur in absence of RGCs although the eye contributes to photoentrainment in such a paradigm. Altogether, our results thus suggest that although phase advances and delays can occur in absence of RGCs, the absence of these cells specifically affect the response to a phase advance paradigm.

To analyze a role for RGCs during masking we calculated the activity of control and *lak* larvae during the pulses of light performed at CT16 and CT21. Interestingly, *lak* larvae showed a reduced level of activity compared to control larvae during the pulse performed at CT16 but not at CT21 further validating that RGCs are involved in masking in the zebrafish larvae but in a circadian dependent manner (CT16 : Fig 2.C, control: 28.33 ± 19.26 mm/min over 10min (n=62), *lak*: 21.45 ± 12.27 mm/min over 10min (n=51); p=0.03; Mann-Whitney two-tailed test; CT21 : Fig 2.F control: 16.51 ± 10.9 mm/min over 10min (n=51), *lak*: 17.17 ± 7.85 mm/min over 10min (n=62); p=0.75).

Condition	**Δphase** Mean±S.D (n)	**P value** Mann-Whitney two-tailed test
DD ctrl	2.34±2.05 (34)	
PD-pulsed ctrl	4.84±1.90 (46)	Ctrl: PD vs DD: ****
PD-pulsed *lak*	5.72±2.32 (37)	PD *lak* vs ctrl: 0.24
PA-pulsed ctrl	-2.61±4.05 (60)	Ctrl: PA vs DD: ****
PA-pulsed *lak*	-0.57±4.1 (25)	PA *lak* vs ctrl: *

Table 1: Quantification of the phase shifts in control versus *lak*-/- (*lak*) larvae kept in DD or submitted to pulses of white light at CT16 or CT21

The Δphase is the difference between the phase of the two last cycles and the phase of the two first cycles. A phase shift is observed in DD owing to the period that is close to 25 hours which generates a ~1 hour-shift every cycle. Upon a pulse of light at CT16 or CT21 a statistical difference is observed between DD and pulsed ctrl larvae as well as *lak* and ctrl larvae when the pulse of light is applied at CT21 (****, p<0,0001; *, p<0,05 using a Mann-Whitney two-tailed test).

opn4xa function is required for endogenous period setting in LL

As circadian rhythms of locomotor activity are established and photoentrain in absence of RGCs, albeit with less efficiency, we wondered if *opn4xa*+ projection neurons present in the pineal gland could play a role in the establishment and photoentrainment of circadian rhythms (Sapède et al., 2020). We, thus, generated a mutant allele for *opn4xa* via CRISPR/Cas9 genome editing using guide RNAs targeting the second coding exon. Amongst various alleles that were generated, we selected an allele that displays a 17 nucleotides insertion for further analysis (Fig 3.A). The protein encoded from this allele is predicted to contain a premature stop codon (Fig 3.B) leading to a truncation of the protein in the middle of the second transmembrane domain (Fig 3.C). As this predicted protein would be devoid of a G protein interaction domain it is assumed to be a null allele. Animals homozygous for this allele were viable and fertile. In addition, *opn4xa*+ cells were present in normal numbers in the retina (Fig 3.D). In the pineal gland, *opn4xa*+ cells express the Wnt effector *tcf7* (Sapède et al., 2020). At 6 days post fertilization, the *opn4xa-/-* pineal gland displays normal expression of *tcf7* (Fig 3.E, WT: 5,5 ± 2,5 (n=4), *opn4xa-/-*: 6± 3 cells (n=3); mean ± S.D). Upon illumination with a 30 min pulse of light, *fos* is expressed in 2-5 cells of the pineal gland which correspond to *opn4xa*+ cells (Fig 3.F, Sapede et al., 2020). On the other hand, *fos* expression is virtually absent in the pineal gland of *opn4xa-/-* embryos after a 30 min pulse of light (Fig 3.F; at 3 days WT: 4,8 ± 0,8 (n=9), *opn4xa-/-*: 0,25 ± 0,7 cells (n=8) per pineal; at 7 days WT: 5,9 ± 3,5 (n=9) *opn4xa-/-*: 0,4 ± 0,7 cells (n=13); mean ± S.D) suggesting that *opn4xa-/-* larvae have lost intrinsic photosensitivity in pineal *opn4xa*+ cells.

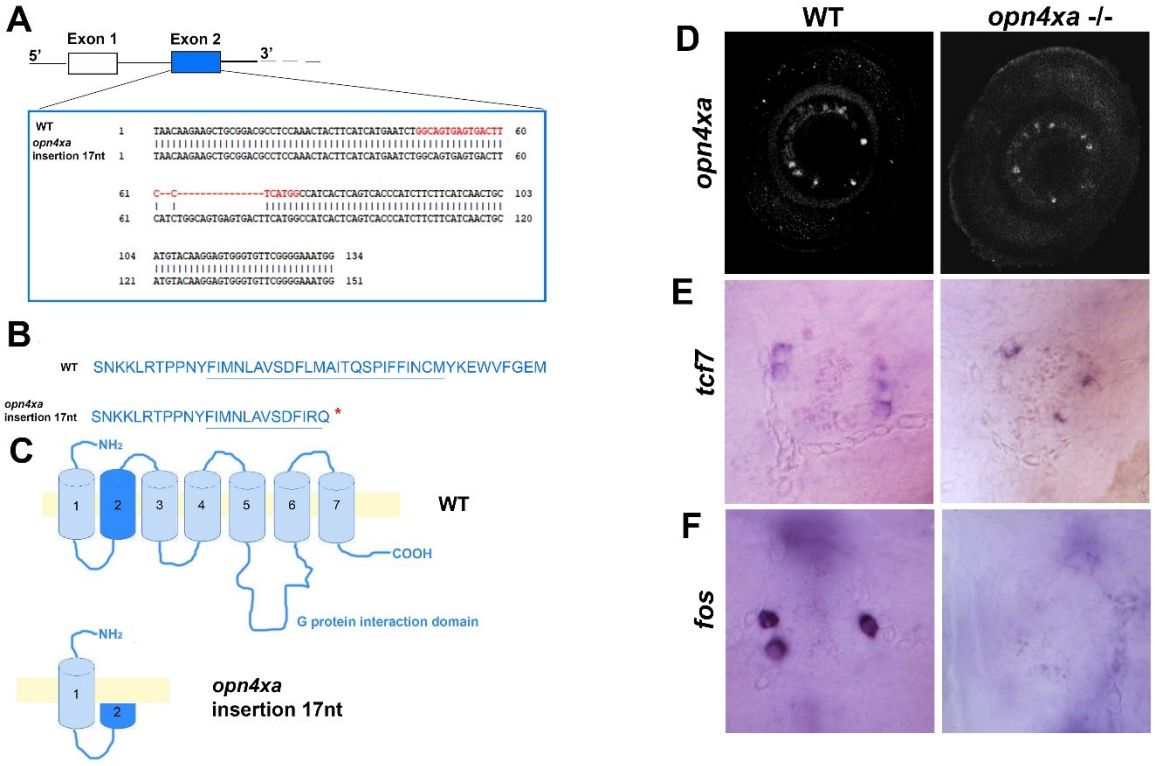

Figure 3: Mutation in *opn4xa* abolishes light sensitivity in pipGCs (A) Scheme showing the 5' part of the *opn4xa* locus and in particular the second exon targeted by the CRISPR guide RNA (target sequence is highlighted in red) as well as the WT and mutant exon2 sequences. (B) Protein sequences produced by the wt and mutant exon 2. The part corresponding to the second transmembrane domain (Matos-Cruz et al., 2011) is underlined. The red asterisk indicates a premature stop codon. (C) Models of the predicted WT and mutant predicted OPN4XA proteins. D) In situ hybridization showing *opn4xa*

expression in the retina at 4 days (E) Expression of *tcf7* in the pineal at 6 days(F) *fos* expression at 3 days.

To determine a role of *opn4xa* in the control of circadian rhythms, we analysed locomotor behaviour of *opn4xa*-/- larvae under various illumination regimes. We found that they still entrained to LD cycles and did not show any difference in levels of locomotor activity as compared to their wild-type siblings (Fig 4.B + supplemental Table 4). In addition, *opn4xa*-/- larvae were able to maintain rhythms of locomotor activity with a similar period as wild-type larvae in DD (Fig 4.C, D). *opn4xa*-/- larvae placed in LL still showed circadian rhythms of locomotor activity (Fig 4.E, F) but with several alterations. First, *opn4xa*-/- larvae were significantly more active during the first night (Supplemental table 6). More importantly, in LL the period was shorter for *opn4xa-/-* larvae compared to controls using both the FFT-NLLS (*opn4xa+/+:* 25.31 ± 3.29 hours (n=66), *opn4xa-/-:* 24.71 ± 3.32 hours (n=66); p=0.041; Mann-Whitney two-tailed test) and mFourfit methods (*opn4xa+/+:* 25.84 ± 1.60 hours (n=66), *opn4xa-/-:* 25.12 ± 1.739 hours (n=66); p=0.012). Altogether these results suggest that *opn4xa* is required for endogenous period setting in LL.

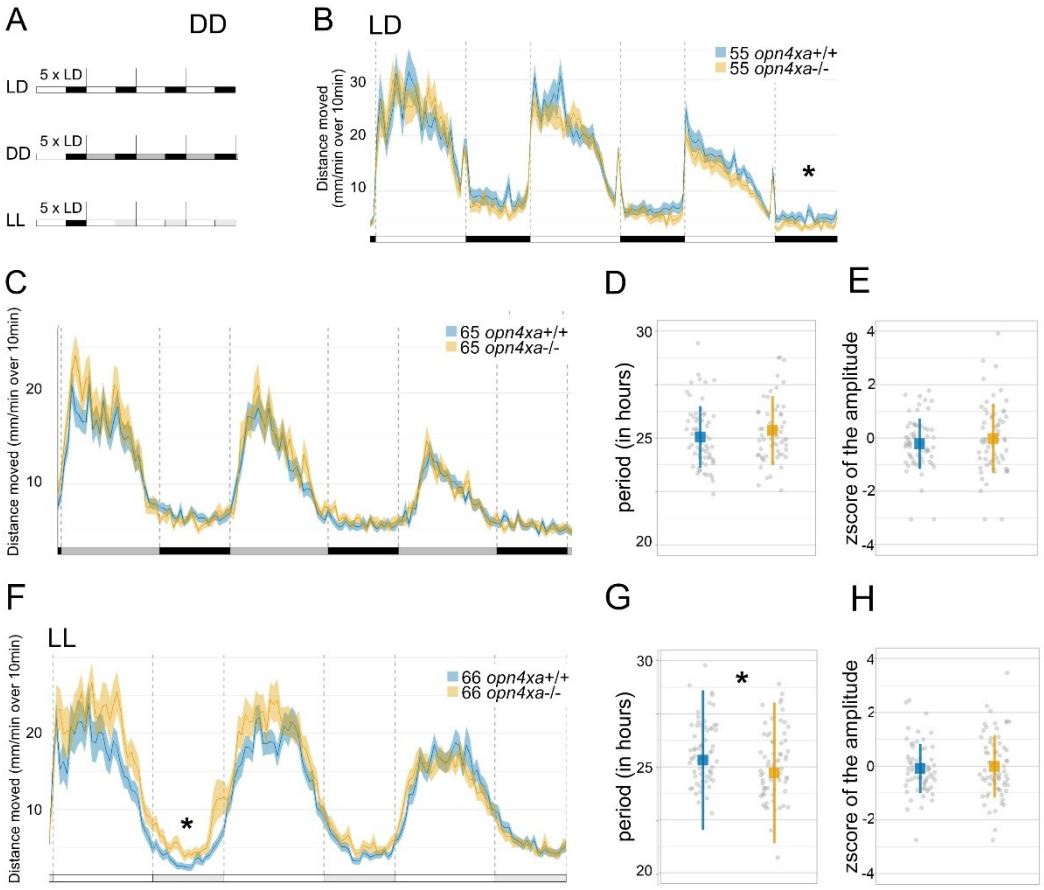

Figure 4: Locomotor activity of larvae devoid of *opn4xa*-mediated photosensitivity (*opn4xa*-/-) in LD, DD and LL

A) Experimental design of LD, DD and LL experiments. White rectangles represent the day period, black rectangles represent the night period, dark grey rectangles represent the subjective day period and light grey rectangles the subjective night. For each experiment, larvae are entrained for 5 LD cycles and their locomotor activity is tracked either in LD (LD), constant darkness (DD) or constant light (LL).

B) Average distance moved (mm/min over 10min) of 3 independent experiments in LD. Mean ± SE. The distance moved is not different in *opn4xa+/+* and *opn4xa-/-* larvae during the 1st (p=0.73), 2nd days (p=0.50) and 3rd days (p=0.07) nor during the 1st (p=0.30), and 2nd nights (p=0.27) (supplemental Table 4). A lower level of activity is found in *opn4xa-/-* larvae during the 3rd night (p=0.01) but is visually clear in only one of the 3 independent experiments (Mann-Whitney two-tailed test).

C) Average distance moved (mm/min over 10min) of 3 independent experiments in DD. Mean ± SE.

D) Estimation of the periods using the FFT-NLLS method calculated over four cycles. The mean period is not significantly different between control and *opn4xa+/+* and *opn4xa-/-* larvae in DD (*opn4xa+/+:* 25.05 ± 1.43 hours (n=64), *opn4xa-/-:* 25.35 ± 1.60 hours (n=60); mean±SD; p=0.29; Mann-Whitney two-tailed test). Mean± sd (in hours) is represented. Each grey point represents a larva.

E) Z-score of the amplitude of circadian rhythm in control and *opn4xa-/-* larvae in DD. Estimation of the amplitude was generated using the FFT-NLLS method. Each grey point represents a single larva. No statistical difference between control and *opn4xa-/-* was observed.

F) Average distance moved (mm/min over 10min) of 4 independent experiments in LL. Mean ± SE. *opn4xa-/-* are more active than controls during the first night (p=0.02, see supplemental Table 6).

G) Estimation of the periods using the FFT-NLLS method calculated over three cycles. The mean period is significantly different between *opn4xa+/+* and *opn4xa-/-* larvae in LL. Mean± sd (in hours) is represented. Each grey point represents a larva.

H) Z-score of the amplitude of circadian rhythm in control and *opn4xa-/-* larvae in LL. Estimation of the amplitude was generated using the FFT-NLLS method on the 4 independent experiments. Each grey point represents a single larva.

***opn4xa* function is dispensable for photoentrainment to a pulse of white light during the subjective night**

We next assessed the ability of pulses of white light at CT 16 and CT21 to induce phase shifts in an *opn4xa-/-* background. We observed that under such conditions *opn4xa-/-* larvae shift their activity to the same extent as their wild-type siblings (Fig 5, Table 3). Furthermore, *opn4xa-/-* larvae did not show any difference in the level of activity during the pulses of light at CT16 or CT21 compared to wildtype siblings, implying that photosensitivity controlled by *opn4xa* is not required for masking (CT16, Fig 5.B, *opn4xa+/+*: 20.30 ± 10.03 mm/min over 10min (n=58), *opn4xa-/-*: 19.42 ± 10.76 mm/min over 10min (n=58); p=0.56; Mann-Whitney two-tailed test. CT21: Fig 5.D, *opn4xa+/+*: 12.85 ± 6.80 mm/min over 10min (n=44), *opn4xa-/-*: 16.54 ± 8.55 mm/min over 10min (n=44); p=0.47). These results show that the intrinsic photosensitivity of *opn4xa* expressing cells is not necessary for circadian photoentrainment or masking.

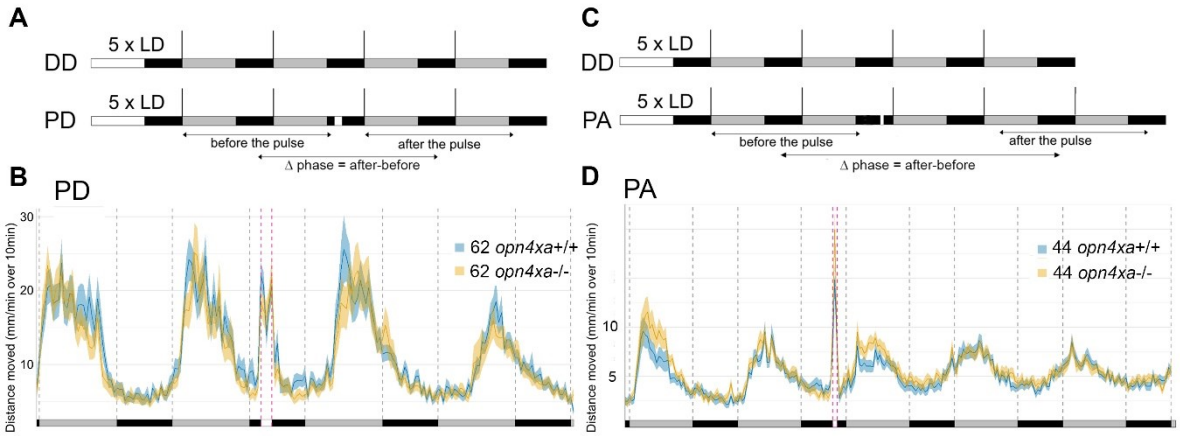

Figure 5: Larvae devoid of *opn4xa*-mediated photosensitivity (*opn4xa-/-*) still photoentrain to pulses of light at CT16 and CT21.

A) Experimental design of phase shift experiments. White rectangles represent the day or light pulse period, black rectangles represent the night period and dark grey rectangles represent the subjective day. For each experiment, larvae are entrained for 5 LD cycles and their locomotor activity is tracked either in constant darkness for 4 days (DD) or tracked in constant darkness for 4 days and subjected to a 2-hours pulse of light during the night of the 2nd day of constant darkness (PD). The phase of locomotor activity is calculated for each larva before and after the timing of the pulse for DD and PS experiments and the △phase (phase after the pulse – phase before the pulse) is calculated.

B) Average distance moved (mm/min over 10min) of 3 independent PD experiments. Mean ± SE. The △phase of *opn4xa+/+* and *opn4xa-/-* larvae calculated with the FFT-NLLS method is not significantly different. *opn4xa*+/+ and *opn4xa-/-*show similar levels of activity during the light pulse (p=0.56, Mann-Whitney two-tailed test).

C) Experimental design of phase advance (PA) experiments. The iconography is similar to A). After 5 training cycles in LD, PA-pulsed larvae were subjected to a one-hour pulse of light at CT21.

D) Average distance moved (mm/min over 10min) of 3 independent PA experiments. Mean ± SE. The △phase of *opn4xa+/+* and *opn4xa-/-* larvae calculated with the FFT-NLLS method is not significantly different (Mann-Whitney two-tailed test).

Condition	**Δphase** Mean±S.D (n)	**P value** Mann-Whitney two-tailed test
DD *opn4xa +/+*	1.64±2.92 (39)	
PD-pulsed *opn4xa +/+*	4.73±2.63 (36)	*opn4xa +/+*: PD vs DD: ****
PD-pulsed *opn4xa -/-*	5.23±4.81 (35)	PD *opn4xa -/-* vs ctrl: 0.32
PA-pulsed *opn4xa +/+*	-2.61±4.05 (60)	*opn4xa +/+*: PA vs DD: ****
PA-pulsed *opn4xa-/-*	-2±2.88 (20)	PA *opn4xa -/-* vs *opn4xa +/+:* 0.39

Table 2: Quantification of the phase shifts in *opn4xa*+/+ versus *opn4xa*-/- larvae kept in DD or submitted to a 2 hours pulse of white light at CT16.

As for table 1, the Δphase is the difference between the phase of the two last cycles and the phase of the two first cycles. A Phase shift is observed in DD owing to the period that is close to 25 hours which generates a ~1 hour-shift every cycle. Phases were calculated with the FFT-NLLS method. Upon a pulse of light at CT16 or CT21 a statistical difference is observed between DD and pulsed ctrl larvae (****, p<0.0001 using a Mann-Whitney two-tailed test). In both phase delays (PD, pulse of light at CT16) and phase advance paradigms (PA, pulse of light at CT21), no statistical difference between ctrl and *opn4xa*-/- is observed using a Mann-Whitney two-tailed test.

Since neither the absence of RGCs (Fig 2) nor the loss of *opn4xa*-dependent photosensitivity (Fig 5) abolishes the capacity of larvae to photoentrain to pulses of light performed in the early or late subjective night, a possible compensation could occur between RGCs and *opn4xa* expressing cells of the pineal gland. To begin addressing this question, we tested photoentrainment properties of *lak-/-; opn4xa-/-* larvae (referred to as 'double'). Compared to *lak* simple mutants, double mutants did not show an attenuated phase shift response to pulses of light at CT16 or CT21 (Fig 6). This suggests that other photosensitive cells mediate photoentrainment in zebrafish.

Finally, *lak* and *lak*/*opn4xa* double mutant larvae show similar levels of activity during the light pulse both at CT 16 and CT21 (CT16: *lak* : 18.23 ± 8.65 mm/min over 10min (n=27), double: 19.79 ± 12.39 mm/min over 10min (n=27); p=0.94, CT21 : *lak*: 17.46 ± 6.65 mm/min over 10min (n=27), double: 16.8 ± 8.05 mm/min over 10min (n=27), p=0.42, Mann-Whitney two-tailed test).

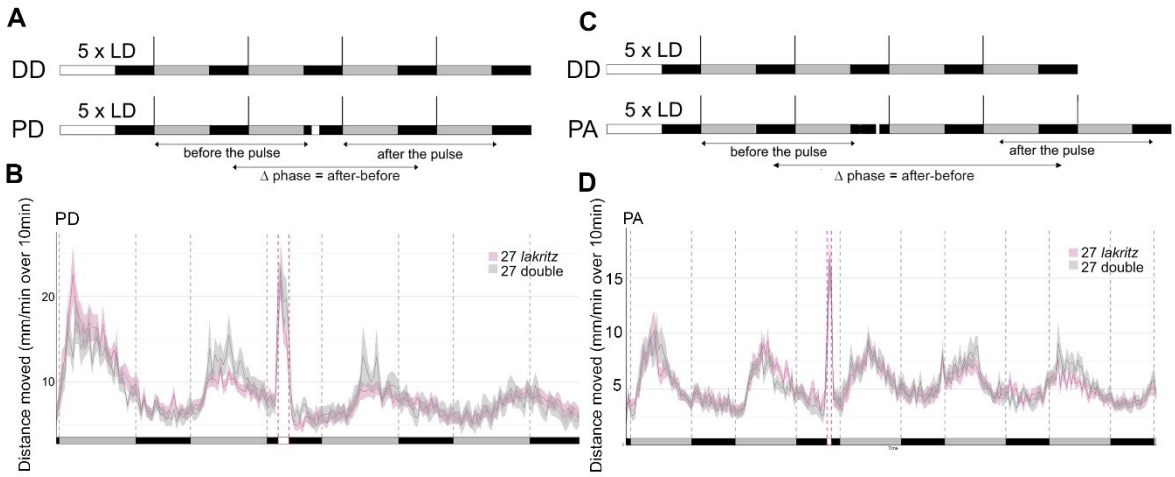

Figure 6: Larvae devoid of RGCs and *opn4xa*-mediated photosensitivity still entrain to pulses of light at CT16 and CT21

A) Experimental design of phase shift experiments. White rectangles represent the day or light pulse period, black rectangles represent the night period and dark grey rectangles represent the subjective day. For each experiment, larvae are entrained for 5 LD cycles and their locomotor activity is tracked either in constant darkness for 4 days (DD) or tracked in constant darkness for 4 days and subjected to a 2-hours pulse of light during the night of the 2nd day of constant darkness (PD). The phase of locomotor activity is calculated for each larva before and after the timing of the pulse for DD and PS experiments and the △phase (phase after the pulse – phase before the pulse) is calculated.

B) Average distance moved (mm/min over 10min) of 3 independent PD experiments (n=27 for *lak* -/- referred as *lak* and n=27 *lak-/-; opn4xa-/-* larvae referred as 'double'). Mean ± SE. The △phase of *lak* and double larvae calculated with the FFT-NLLS method are not significantly different (see table 3).

C) Experimental design of phase advance (PA) experiments. The iconography is similar to A). After 5 training cycles in LD, PA-pulsed larvae were subjected to a one-hour pulse of light at CT21.

D) Average distance moved (mm/min over 10min) of 3 independent PA experiments (n=27 for *lak* and n=27 double larvae). Error bars represent SE. The △phase of *lak* and double larvae calculated with the FFT-NLLS method are not significantly different (see table 3).

Condition	**Δphase** Mean±S.D (n)	**P value** Mann-Whitney two-tailed test
DD *lak*	2.082±2.24 (35)	
PD-pulsed *lak*	5.72±2.32 (37)	*lak*: PD vs DD: ****
PD-pulsed double	4.90±2.23 (14)	PD double vs *lak*: 0.33
PA-pulsed *lak*	-0.59±4.10 (25)	*lak*: PA vs DD:****
PA-pulsed double	-3.14±5.25 (14)	PA double vs *lak* : 0.42

Table 3: Quantification of the phase shifts in WT (*opn4xa*+/+) versus *opn4xa*-/- larvae kept in DD or submitted to a 2 hours pulse of white light at CT16.

As for table 1 and 2, the Δphase is the difference between the phase of the two last cycles and the phase of the two first cycles. A Phase shift is observed in DD owing to the period that is close to 25 hours which generates a ~1 hour-shift every cycle. Phases were calculated with the FFT-NLLS method (biodare2.ed.ac.uk). Upon a pulse of light at CT16 or CT21 a statistical difference is observed between DD and pulsed *lak* larvae (****. p<0.0001 using a Mann-Whitney two-tailed test). In both phase delays (PD, pulse of light at CT16) and phase advance paradigms (PA. pulse of light at CT21), no statistical difference between *lak* and double larvae is observed using a Mann-Whitney two-tailed test.

Discussion

Melanopsin expressing RGCs have been thought to be the sole mediators of masking and photoentrainment of locomotor activity for a long time. Here, we show that in contrast to this belief that was fostered by functional observations made in nocturnal rodents, circadian rhythms of locomotor activity are established and photoentrain in the absence of RGCs in zebrafish larvae. Furthermore, our results strongly suggest that the absence of a functional eye affects masking, but in a circadian dependent manner. As zebrafish also possesses melanopsin expressing cells in their pineal gland (Sapède et al.. 2020), we engineered an *opn4xa* mutant line to address the role of *opn4xa*-dependent photosensitivity in this structure. Our data suggests that *opn4xa* is neither involved in masking nor in the establishment/photoentrainment of circadian rhythms. While our analysis does not support a redundant role for RGCs and *opn4xa* photosensitivity during photoentrainment of circadian rhythms it reveals a subtle function of *opn4xa*-dependent photosensitivity, possibly in the pineal, in the control the period length of circadian rhythms in constant light.

Subtle defects in *opn4xa-/-* and *lak* mutants in LL

While no differences in period or amplitude of locomotor rhythms are observed for *lak* and *opn4xa* mutant larvae in DD, subtle alterations are observed in LL. Abrogation of *opn4xa* activity reduces the increase of period length observed when larvae are placed in LL. A similar defect is observed in *Opn4*-/- mice placed in constant light condition (Panda et al.. 2002; Ruby et al.. 2002) suggesting this could be a conserved function of melanopsin. Interestingly, this phenotype is not observed in *lak* mutant suggesting that in zebrafish this melanopsin function might involve the pineal rather than the eye. Our results also suggest that the eye, but not *opn4xa*-dependent photosensitivity,

controls the amplitude of circadian rhythmicity in LL. Surprisingly, both the effect of mutations in *opn4xa* on the period and of mutations in *lak* on the amplitude of circadian rhythms are observed in LL but not in DD. This could be linked to a greater instability of the circadian clock in LL compared to DD as described in *Drosophila* (Emery et al., 2000). Along this line, it is noteworthy that the variation observed for both the period and the level of activity are higher in LL than in DD for both control and mutant larvae. We propose that in constant light the zebrafish circadian system functions less robustly and is more prone to subtle destabilization in mutant contexts.

RGCs, but not *opn4xa*, are involved in masking

Compared to their control siblings, we found *lak* mutant larvae to be less active during the light phases of LD cycles as well as when subjected to a pulse of light at CT16 but not at CT21. This reveals a role for RGCs in positive masking in zebrafish larvae as well as a circadian control of this masking activity. In contrast, *opn4xa*-/- larvae display no defect in masking of locomotor activity in LD or during a pulse of light suggesting that *opn4xa*-dependent photosensitivity is dispensable for this type of masking. Moreover, masking is not completely abolished in *lak* mutant larvae. In addition, *lak*;*opn4xa* double mutants show a similar activity to *lak*-/- larvae during a pulse of light at CT16 and CT21, suggesting that there is no redundancy between the eye and *opn4xa*+ cells in the pineal for masking control. Other photosensitive cells are thus involved in this process. Among these could be the classical photoreceptors of the pineal or deep brain photoreceptors, such as those involved in the locomotor response to a loss of illumination (Fernandes et al.. 2012).

RGCs and *opn4xa* are largely dispensable for shifting circadian rhythms of locomotor activity in response to a pulse of white light

The present study shows that neither the eye nor *opn4xa* mediated photosensitivity in the pineal gland is absolutely required for the development of circadian rhythms and circadian photoentrainment. The absence of a strong requirement for the eye to control the circadian system in zebrafish is surprising given that *Astyanax mexicanus* blind cavefishes are arrhythmic in DD (Beale et al.. 2013) while *Phreatichthys andruzzii* adult cavefishes, which also exhibit a complete eye degeneration, and are arrhythmic in LD when fed at random times (Cavallari et al.. 2011). In light of our data, we propose that apart from the eye, other photosensitive structures might be affected in these other fish species. This in turn begs the question as to which structure(s) relay light information to control circadian rhythm in fishes and other non-mammalian animals? The pineal gland, with its classical photoreceptors and *opn4xa*+ projection neurons is an appealing candidate (Sapède and Cau. 2013). Strategies aiming at genetically killing this structure or impairing its activity will surely help unravelling its function. Studies describing the effect of surgical pinealectomy have been reported in a number of non-mammalian vertebrates. The phenotypes induced seem to depend strongly on the species. For instance, pinealectomy abolishes rhythms in the stinging catfish but not in the amur catfish or the lake chub. Interestingly, in species where rhythms are maintained upon pinealectomy a change in period can occur (see (Zhdanova and Reebs, 2005) for a review). A similar variety of phenotypes are induced upon pinealectomy in reptiles or birds. In addition to the pineal gland, reptiles have a parietal eye, a structure that is developmentally and spatially related to the pineal gland. Interestingly simultaneous removal of the eye, the pineal gland and the parietal eye in two species of lizards (*P. Sicula* and *S. olivaceous*), does not impair rhythms of locomotor activity while on the contrary these rhythms are lost if in addition to this triple ablation injection of dark ink between the skin and the skull is performed (Tosini et al.. 2001). Similarly, experiments in songbirds suggest the existence of additional photosensitive structures located in the brain that control photoentrainment (Menaker and Underwood. 1976). Altogether these results highlight the existence of other brain structures mediating light inputs on the circadian system. Interestingly, melanopsin expression has been described in other brain areas in the zebrafish larva: *opn4a* is expressed within the presumptive optic area, *opn4b* is found in the ventral forebrain and the thalamic region, and *opn4.1* is detected in a specific domain located in the ventricular region at the junction between the caudal hindbrain and the

anterior spinal cord (Fernandes et al.. 2012; Matos-Cruz et al.. 2011). Larvae double mutant for *opn4.1* and *opn4xb* do not exhibit a circadian phenotype (Dekens et al., 2022). As 42 opsin genes are predicted in the zebrafish genome, of which 20 are expressed in the adult brain (Davies et al.. 2015), further characterization of their expression in the larval brain will be needed to define the best candidates for further study. Finally, the possibility remains that photoentrainment in zebrafish occurs as a result of direct photosensitivity of motoneurons or muscles themselves as all cells and organs have been shown to be directly photosensitive and light-entrainable in this species (see (Vatine et al.. 2011) for a review).

Taken together, our results highlight profound differences in the establishment and photoentrainment of the circadian system between the diurnal zebrafish and the nocturnal rodents. A crucial, yet open question is whether these divergences reflect the different phylogeny of these species or their different use of temporal niches. The photosensitive capabilities of the zebrafish in particular and of aquatic species in general (as judged by the number of opsins predicted in the genome) far exceed that observed in mammals. This could imply a greater level of complexity and robustness in circadian control in zebrafish independently of its temporal niche. However, the human brain also expresses opsins (*OPN3* and *OPN5*; (Halford et al., 2001; Tarttelin et al., 2003)) suggesting the existence of deep brain photoreceptors in diurnal primates and the possibility that they participate in photoentrainment.

Declaration of competing interest

The authors declare that no competing interests exist.

Acknowledgements

We are indebted to C. Rampon for allowing us to use the Ethovision Software. We thank M. Halpern and K. Soanes for sharing probes and to members of the Blader team for helpful discussions. This work was supported by the Centre National de la Recherche Scientifique (CNRS); the Institut National de la Santé et de la Recherche Médicale (INSERM); Université de Toulouse III (UPS); Fondation pour la Recherche Médicale (FRM; DEQ20131029166); Fédération pour la Recherche sur le Cerveau (FRC); Association pour la Recherche sur le Cancer (ARC); Association Rétina France and the Ministère de la Recherche. We would like to thank Brice Ronsin, Stéphanie Bosch and the Toulouse RIO Imaging platform; Stéphane Relexans, Aurore Laire and Richard Brimicombe for taking care of the fish as well as Sophie Polès for technical help.

MATERIAL AND METHODS

Zebrafish lines and developmental conditions

All animals were handled in the CBI fish facility, which is certified by the French Ministry of Agriculture (approval number A3155510). The project was approved by the French Ministry of Teaching and Research (agreement number APAFIS#3653-2.016.011.512.005.922). Embryos were reared at 28 degrees in a 14h light:10h dark cycle with lights on at 9:00 and lights off at 23:00.

The *lak* mutant line has been described previously (Kay et al.. 2001), *lak* homozygous mutants were identified by their dark coloration. The protocol for genotyping *lak* individuals is available upon request.

To genotype *opn4xa* individuals, we used a classical PCR protocol with the following oligos: 5'-GGACGCCTCCAAACTTC-3' (Forward) and 5'-CGAACACCCACTCCTTGTAC-3' Reverse). PCR products of different sizes were obtained (110bp for the wt allele and 127bp for the mutant allele) and resolved on a 4% agarose gel.

Generation of an *opn4xa* mutant allele

An *opn4xa* mutant allele was generated using the CRISPR/ Cas9 targeted genome editing. For this. a target site was designed in the second exon by manual screening for PAM sites. Transcription of the

guide and coinjection of the guide mRNA with cas9 mRNA was performed as described in (Lekk et al.. 2019). Screening of potential mutants was performed using T7 endonuclease (NEB) treatment of PCR products amplifying the second *opn4xa* exon (Fw : 5' CACAACATAAACTGTAACTGCATCC 3', Rev : 5' GACACGGGTATGACACTCAGGAAGG 3'). PCR products from potential carriers were subsequently subcloned and sequenced. In this manner we identified several interesting carriers among which an individual transmitting an allele bearing 17 extra nucleotides in the second exon leading to a premature interruption of the coding sequence.

For further experiments. *opn4xa* mutant animals were genotyped using a short PCR product centered on the second exon run on a 4 % gel which allows to see the 17 nt difference between the two alleles.

Locomotor Activity Assays

Larvae zebrafish coming from heterozygous incrosses were raised on a 14:10 hr light:dark cycle at 28°C in Petri dishes with no more than 50 larvae per Petri dish in a water bath inside the fish facility. On the morning of their 5th day of development (9:15-10:30), individual larvae were placed in each well of a 96-well plate (Whatman® UNIPLATE. 105x69mm) containing aquarium fish water and placed back in the water bath. On the evening (16:00-20:00), the plate was put in an hermetic box in a dark room maintained at approximately 27°C with a heater. The box was continuously illuminated from below with two panels of infra-red lights as well as white light controlled by a timer (280 lux at water surface) from 9:00 to 23:00. Larvae were then filmed at 30 frames per second, with a ceiling mounted infra-red camera connected to a computer on the following days (from the 6th day of development to the 9th or 10th day of development) in controlled conditions of illumination. The temperature inside the box was monitored using an electronic programmable device (I Button. Maxim). After the experiment, larvae were either genotyped by PCR for *opn4xa* and/or *lak* and/or simply identified for the *lak* mutation using the dark coloration phenotype. In addition, larvae presenting developmental defects were discarded from the subsequent analysis. Experiments in which too many larvae presented development issues or where temperature issues were present were discarded. At least three experiments were made for each type of assay.

In Situ Hybridization

In situ hybridization was performed as described previously (Cau et al.. 2008). *opn4xa, tcf7* and *c-fos* probes have been described previously (Matos-Cruz et al.,2011; Ellis et al.,2012; Sapède et al., 2020).

Locomotor Activity Analysis

After the experiment, the distance travelled per minute was extracted for each larva using the Ethovision XT13.0 (Noldus. Wageningen. the Netherlands) with the following parameters: for Detection Settings: dynamic substraction ; subject color compared to background : Darker ; Dark : 7 to 210 ; Frame Weight : 2 ; for Track Smoothing Profiles :Minimal Distance Moved : 0.2mm - Direct (A>MDM) ; for Data Profiles : Results per time bin. Ignore last time bin if incomplete; for Analysis Profiles: Distance moved of the center-point. The obtained files were then analysed using the wakefish program (written in python by L.Sanchou) to extract an average activity of mm/min over 10min for each larva ('DM10 files'). For each experiment, the same number of homozygous mutants and wild-type or control larvae were randomly selected. The Biodare software was used to calculate periods and phases for each larva (biodare2.ed.ac.uk). We choose to use the FFT-NLLS to calculate periods and phases on DM10 files after baseline detrending, as advised (Zielinski et al., 2014). The parameters used for period calculation were as follows: baseline detrending, expected periods from 18 to 30 hours. analysis method FFT-NLLS. To calculate the amplitude, we used the same method but no detrending as this filtering could affect the amplitude. The parameters used for phase calculation were as follows: baseline detrending. FFT-NLLS, phase by fit, absolute phase to window. Windows used to calculate the phase of locomotor activity "before the pulse" and "after the pulse" encompass time points from CT0 to CT15 (corresponding from 9am of the 1st day in of the experiment to midnight between the 2nd and

3rd day of the experiment for "before the pulse" and from 9am of the 3rd day of the experiment to midnight between the 4th and 5th day of the experiment). Locomotor activity levels were calculated from the DM10 files by calculating means of the average activity in mm/min over 10 min over a given period for each larva. Statistical analysis was done using Prism. Graphs were generated using R studio (ggplot2 and rethomics packages (Geissmann et al., 2019; Wickham, 2016)).

REFERENCES

Altimus, C.M., Güler, A.D., Villa, K.L., McNeill, D.S., Legates, T.A., and Hattar, S. (2008). Rods-cones and melanopsin detect light and dark to modulate sleep independent of image formation. Proc. Natl. Acad. Sci. U. S. A. *105*, 19998–20003. https://doi.org/10.1073/pnas.0808312105.

Bailes, H.J., and Lucas, R.J. (2010). Melanopsin and inner retinal photoreception. Cell. Mol. Life Sci. *67*, 99–111. https://doi.org/10.1007/s00018-009-0155-7.

Baver, S.B., Pickard, G.E., Sollars, P.J., and Pickard, G.E. (2008). Two types of melanopsin retinal ganglion cell differentially innervate the hypothalamic suprachiasmatic nucleus and the olivary pretectal nucleus. Eur. J. Neurosci. *27*, 1763–1770. https://doi.org/https://doi.org/10.1111/j.1460-9568.2008.06149.x.

Beale, A., Guibal, C., Tamai, T.K., Klotz, L., Cowen, S., Peyric, E., Reynoso, V.H., Yamamoto, Y., and Whitmore, D. (2013). Circadian rhythms in Mexican blind cavefish Astyanax mexicanus in the lab and in the field. Nat. Commun. *4*, 1–10. https://doi.org/10.1038/ncomms3769.

Belenky, M.A., Smeraski, C.A., Provencio, I., Sollars, P.J., and Pickard, G.E. (2003). Melanopsin retinal ganglion cells receive bipolar and amacrine cell synapses. J. Comp. Neurol. *460*, 380–393. https://doi.org/https://doi.org/10.1002/cne.10652.

Bhadra, B., N, T., P, D., and M, P.B. (2017). Evolution of circadian rhythms: from bacteria to human.

Brzezinski, J.A., Brown, N.L., Tanikawa, A., Bush, R.A., Sieving, P.A., Vitaterna, M.H., Takahashi, J.S., and Glaser, T. (2005). Loss of Circadian Photoentrainment and Abnormal Retinal Electrophysiology in Math5 Mutant Mice. Invest. Ophthalmol. Vis. Sci. *46*, 2540–2551. https://doi.org/10.1167/iovs.04-1123.

Cahill, G.M. (1996). Circadian regulation of melatonin production in cultured zebrafish pineal and retina. Brain Res. *708*, 177–181. https://doi.org/10.1016/0006-8993(95)01365-2.

Calligaro, H., Coutanson, C., Najjar, R.P., Mazzaro, N., Cooper, H.M., Haddjeri, N., Felder-Schmittbuhl, M.-P., and Dkhissi-Benyahya, O. (2019). Rods contribute to the light-induced phase shift of the retinal clock in mammals. PLoS Biol. *17*, e2006211. https://doi.org/10.1371/journal.pbio.2006211.

Cau, E., Quillien, A., and Blader, P. (2008). Notch resolves mixed neural identities in the zebrafish epiphysis. Dev. Camb. Engl. *135*, 2391–2401. https://doi.org/10.1242/dev.013482.

Cavallari, N., Frigato, E., Vallone, D., Fröhlich, N., Lopez-Olmeda, J.F., Foà, A., Berti, R., Sánchez-Vázquez, F.J., Bertolucci, C., and Foulkes, N.S. (2011). A Blind Circadian Clock in Cavefish Reveals that Opsins Mediate Peripheral Clock Photoreception. PLoS Biol. *9*. https://doi.org/10.1371/journal.pbio.1001142.

Chew, K.S., Renna, J.M., McNeill, D.S., Fernandez, D.C., Keenan, W.T., Thomsen, M.B., Ecker, J.L., Loevinsohn, G.S., VanDunk, C., Vicarel, D.C., et al. (2017). A subset of ipRGCs regulates both

maturation of the circadian clock and segregation of retinogeniculate projections in mice. eLife *6*, e22861. https://doi.org/10.7554/eLife.22861.

Covello, G., Rossello, F.J., Filosi, M., Gajardo, F., Duchemin, A., Tremonti, B.F., Eichenlaub, M., Polo, J.M., Powell, D., Ngai, J., et al. (2020). Transcriptome analysis of the zebrafish atoh7−/− Mutant, lakritz, highlights Atoh7-dependent genetic networks with potential implications for human eye diseases. FASEB BioAdvances *2*, 434–448. https://doi.org/10.1096/fba.2020-00030.

Davies, W.I.L., Tamai, T.K., Zheng, L., Fu, J.K., Rihel, J., Foster, R.G., Whitmore, D., and Hankins, M.W. (2015). An extended family of novel vertebrate photopigments is widely expressed and displays a diversity of function. Genome Res. *25*, 1666–1679. https://doi.org/10.1101/gr.189886.115.

Dekens, M.P.S., Fontinha, B.M., Gallach, M., Pflügler, S., and Tessmar-Raible, K. (2022). Melanopsin elevates locomotor activity during the wake state of the diurnal zebrafish. EMBO Rep. *23*, e51528. https://doi.org/10.15252/embr.202051528.

Dibner, C., Schibler, U., and Albrecht, U. (2010). The Mammalian Circadian Timing System: Organization and Coordination of Central and Peripheral Clocks. Annu. Rev. Physiol. *72*, 517–549. https://doi.org/10.1146/annurev-physiol-021909-135821.

Dkhissi-Benyahya, O., Gronfier, C., De Vanssay, W., Flamant, F., and Cooper, H.M. (2007). Modeling the role of mid-wavelength cones in circadian responses to light. Neuron *53*, 677–687. https://doi.org/10.1016/j.neuron.2007.02.005.

Dollet, A., Albrecht, U., Cooper, H.M., and Dkhissi-Benyahya, O. (2010). Cones Are Required for Normal Temporal Responses to Light of Phase Shifts and Clock Gene Expression. Chronobiol. Int. *27*, 768–781. https://doi.org/10.3109/07420521003695704.

Emery, P., Stanewsky, R., Hall, J.C., and Rosbash, M. (2000). A unique circadian-rhythm photoreceptor. Nature *404*, 456–457. https://doi.org/10.1038/35006558.

Fernandes, A.M., Fero, K., Arrenberg, A.B., Bergeron, S.A., Driever, W., and Burgess, H.A. (2012). Deep brain photoreceptors control light seeking behavior in zebrafish larvae. Curr. Biol. CB *22*, 2042–2047. https://doi.org/10.1016/j.cub.2012.08.016.

Fernandez, D.C., Chang, Y.-T., Hattar, S., and Chen, S.-K. (2016). Architecture of retinal projections to the central circadian pacemaker. Proc. Natl. Acad. Sci. *113*, 6047–6052. .

Freedman, M.S., Lucas, R.J., Soni, B., Schantz, M. von, Muñoz, M., David-Gray, Z., and Foster, R. (1999). Regulation of Mammalian Circadian Behavior by Non-rod, Non-cone, Ocular Photoreceptors. Science https://doi.org/10.1126/science.284.5413.502.

Geissmann, Q., Rodriguez, L.G., Beckwith, E.J., and Gilestro, G.F. (2019). Rethomics: An R framework to analyse high-throughput behavioural data. PLOS ONE *14*, e0209331. https://doi.org/10.1371/journal.pone.0209331.

Güler, A.D., Ecker, J.L., Lall, G.S., Haq, S., Altimus, C.M., Liao, H.-W., Barnard, A.R., Cahill, H., Badea, T.C., Zhao, H., et al. (2008). Melanopsin cells are the principal conduits for rod-cone input to non-image-forming vision. Nature *453*, 102–105. https://doi.org/10.1038/nature06829.

Halford, S., Freedman, Melanie S., Bellingham, J., Inglis, S.L., Poopalasundaram, S., Soni, B.G., Foster, R.G., and Hunt, D.M. (2001). Characterization of a Novel Human Opsin Gene with Wide Tissue

Expression and Identification of Embedded and Flanking Genes on Chromosome 1q43. Genomics *72*, 203–208. https://doi.org/10.1006/geno.2001.6469.

Kay, J.N., Finger-Baier, K.C., Roeser, T., Staub, W., and Baier, H. (2001). Retinal Ganglion Cell Genesis Requires lakritz, a Zebrafish atonal Homolog. Neuron *30*, 725–736. https://doi.org/10.1016/S0896-6273(01)00312-9.

Kofuji, P., Mure, L.S., Massman, L.J., Purrier, N., Panda, S., and Engeland, W.C. (2016). Intrinsically Photosensitive Retinal Ganglion Cells (ipRGCs) Are Necessary for Light Entrainment of Peripheral Clocks. PLOS ONE *11*, e0168651. https://doi.org/10.1371/journal.pone.0168651.

Kölsch, Y., Hahn, J., Sappington, A., Stemmer, M., Fernandes, A.M., Helmbrecht, T.O., Lele, S., Butrus, S., Laurell, E., Arnold-Ammer, I., et al. (2021). Molecular classification of zebrafish retinal ganglion cells links genes to cell types to behavior. Neuron *109*, 645–662.e9. https://doi.org/10.1016/j.neuron.2020.12.003.

Lekk, I., Duboc, V., Faro, A., Nicolaou, S., Blader, P., and Wilson, S.W. (2019). Sox1a mediates the ability of the parapineal to impart habenular left-right asymmetry. eLife *8*, e47376. https://doi.org/10.7554/eLife.47376.

Li, J.Y., and Schmidt, T.M. (2018). Divergent projection patterns of M1 ipRGC subtypes. J. Comp. Neurol. *526*, 2010–2018. https://doi.org/10.1002/cne.24469.

Matos-Cruz, V., Blasic, J., Nickle, B., Robinson, P.R., Hattar, S., and Halpern, M.E. (2011). Unexpected diversity and photoperiod dependence of the zebrafish melanopsin system. PloS One *6*, e25111. https://doi.org/10.1371/journal.pone.0025111.

Menaker, M., and Underwood, H. (1976). Extraretinal Photoreception in Birds. Photochem. Photobiol. *23*, 299–306. https://doi.org/https://doi.org/10.1111/j.1751-1097.1976.tb07251.x.

Neuhauss, S.C.F., Biehlmaier, O., Seeliger, M.W., Das, T., Kohler, K., Harris, W.A., and Baier, H. (1999). Genetic Disorders of Vision Revealed by a Behavioral Screen of 400 Essential Loci in Zebrafish. J. Neurosci. *19*, 8603–8615. https://doi.org/10.1523/JNEUROSCI.19-19-08603.1999.

Noche, R.R., Lu, P.-N., Goldstein-Kral, L., Glasgow, E., and Liang, J.O. (2011). Circadian rhythms in the pineal organ persist in zebrafish larvae that lack ventral brain. BMC Neurosci. *12*, 7. https://doi.org/10.1186/1471-2202-12-7.

Panda, S., Sato, T.K., Castrucci, A.M., Rollag, M.D., DeGrip, W.J., Hogenesch, J.B., Provencio, I., and Kay, S.A. (2002). Melanopsin (Opn4) requirement for normal light-induced circadian phase shifting. Science *298*, 2213–2216. https://doi.org/10.1126/science.1076848.

Perez-Leon, J.A., Warren, E.J., Allen, C.N., Robinson, D.W., and Brown, R.L. (2006). Synaptic inputs to retinal ganglion cells that set the circadian clock. Eur. J. Neurosci. *24*, 1117–1123. https://doi.org/10.1111/j.1460-9568.2006.04999.x.

Ruby, N.F., Brennan, T.J., Xie, X., Cao, V., Franken, P., Heller, H.C., and O'Hara, B.F. (2002). Role of melanopsin in circadian responses to light. Science *298*, 2211–2213. https://doi.org/10.1126/science.1076701.

Rupp, A.C., Ren, M., Altimus, C.M., Fernandez, D.C., Richardson, M., Turek, F., Hattar, S., and Schmidt, T.M. (2019). Distinct ipRGC subpopulations mediate light's acute and circadian effects on body temperature and sleep. eLife *8*, e44358. https://doi.org/10.7554/eLife.44358.

Sapède, D., and Cau, E. (2013). The pineal gland from development to function. Curr. Top. Dev. Biol. *106*, 171–215. https://doi.org/10.1016/B978-0-12-416021-7.00005-5.

Sapède, D., Chaigne, C., Blader, P., and Cau, E. (2020). Functional heterogeneity in the pineal projection neurons of zebrafish. Mol. Cell. Neurosci. *103*, 103468. https://doi.org/10.1016/j.mcn.2020.103468.

Tamai, T.K., Young, L.C., and Whitmore, D. (2007). Light signaling to the zebrafish circadian clock by Cryptochrome 1a. Proc. Natl. Acad. Sci. U. S. A. *104*, 14712–14717. https://doi.org/10.1073/pnas.0704588104.

Tarttelin, E.E., Bellingham, J., Hankins, M.W., Foster, R.G., and Lucas, R.J. (2003). Neuropsin (Opn5): a novel opsin identified in mammalian neural tissue 1. FEBS Lett. *554*, 410–416. https://doi.org/https://doi.org/10.1016/S0014-5793(03)01212-2.

Tosini, G., Bertolucci, C., and Foà, A. (2001). The circadian system of reptiles: a multioscillatory and multiphotoreceptive system. Physiol. Behav. *72*, 461–471. https://doi.org/10.1016/S0031-9384(00)00423-6.

Vallone, D., Gondi, S.B., Whitmore, D., and Foulkes, N.S. (2004). E-box function in a period gene repressed by light. Proc. Natl. Acad. Sci. U. S. A. *101*, 4106–4111. https://doi.org/10.1073/pnas.0305436101.

Vatine, G., Vallone, D., Gothilf, Y., and Foulkes, N.S. (2011). It's time to swim! Zebrafish and the circadian clock. FEBS Lett. *585*, 1485–1494. https://doi.org/10.1016/j.febslet.2011.04.007.

Wee, R., Castrucci, A.M., Provencio, I., Gan, L., and Van Gelder, R.N. (2002). Loss of Photic Entrainment and Altered Free-Running Circadian Rhythms in math5−/− Mice. J. Neurosci. *22*, 10427–10433. .

Wickham, H. (2016). ggplot2: Elegant Graphics for Data Analysis. Springer-Verl. N. Y. ISBN 978-3-319-24277-4.

Wong, K.Y., Dunn, F.A., Graham, D.M., and Berson, D.M. (2007). Synaptic influences on rat ganglion-cell photoreceptors. J. Physiol. *582*, 279–296. https://doi.org/10.1113/jphysiol.2007.133751.

Zhdanova, I.V., and Reebs, S.G. (2005). Circadian Rhythms in Fish. Fish Physiol. Acad. Press 197–238. .

Supplemental data:

Suplemental figure 1:

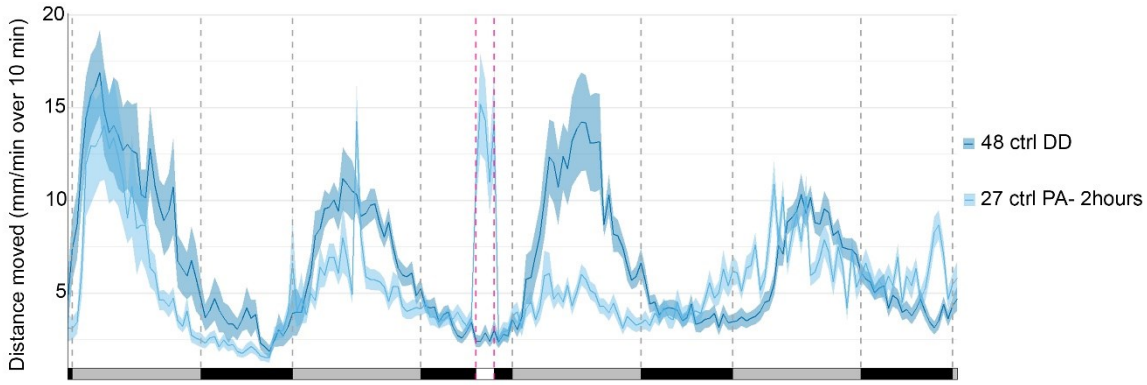

Average distance moved of control larvae (mm/min over 10min) in 2 independent DD experiments and 1 PA experiment. For the PA experiment the larvae were subjected to a 2 hours pulse of white light at CT20. Mean ± SE.

Legend for the following supplemental tables :

Tables showing the average distance travelled (mm/min) over a 10 min window averaged during the day (D) or the night (N) periods. D1 corresponds to the first day. The p value and statistical significance using a two-tailed Mann-Whitney test is indicated.

Supplemental table 1: activity of *lakritz* -/- versus control larvae in LD

condition	ctrl (n=55)	*lakritz* (n=55)	p value
D1	13.95 ± 9.76	9.72 ± 8.73	** **0.008**
N1	2.92 ± 2.28	2.85 ± 2.57	n.s 0.42
D2	16.90 ± 10.25	11.18 ± 7.40	*** **0.0005**
N2	4.04 ± 2.22	4.98 ± 4.22	n.s 0.51
D3	13.19 ± 8.56	10.88 ± 7.07	n.s 0.13
N3	3.56 ± 2.17	3.95 ± 2.94	n.s 0.57

Supplemental table 2: activity of *lakritz* -/- versus control larvae in DD

condition	ctrl (n=48)	*lakritz* (n=48)	p value
D1	11.16 ± 10.86	10.83 ± 8.36	n.s 0.82
N1	3.37 ± 4.31	2.70 ± 2.02	n.s 0.76
D2	7.91 ± 4.29	8.67 ± 6.64	n.s 0.85
N2	3.26 ± 1.50	3.44 ± 2.14	n.s 0.90
D3	9.37 ± 8.63	9.32 ± 6.33	n.s 0.76
N3	4.07 ± 1.83	4 ± 2.45	n.s 0.40
D4	6.94 ± 2.99	6.27 ± 3.29	n.s 0.05
N4	4.48 ± 2.11	4.33 ± 2.32	n.s 0.50

Supplemental table 3: activity of *lakritz* -/- versus control larvae in LL

condition	ctrl (n=81)	*lakritz* (n=81)	p value
D1	34.18 ± 21.69	37.37 ± 26.95	n.s 0.50
N1	17.90 ± 15.82	22.74 ± 20.38	n.s 0.42
D2	36.10 ± 19.08	35.57 ± 23.48	n.s 0.61
N2	21.18 ± 18.32	24.91 ± 21.59	n.s 0.47
D3	30.03 ± 17.35	30.59 ± 20.83	n.s 0.91
N3	17.76 ± 15.52	21.76 ± 19.23	n.s 0.48

Supplemental table 4: activity of *opn4xa* -/- versus control larvae in LD

condition	wt (n=48)	*opn4xa-/-* (n=48)	p value
D1	22.16 ± 10.02	22.42 ± 13.12	n.s 0.73
N1	9.41 ± 6.45	7.94 ± 4.99	n.s 0.30
D2	20.46 ± 7.96	19.49 ± 8.25	n.s 0.50
N2	7.27 ± 4.86	6.32 ± 4.53	n.s 0.27
D3	14.35 ± 5.19	12.52 ± 6.12	n.s 0.07
N3	5.59 ± 3.41	4.19 ± 3.09	*** 0.01**

Supplemental table 5: activity of *opn4xa* -/- versus control larvae in DD

condition	wt (n=65)	*opn4xa-/-* (n=65)	p value
D1	14.73 ± 7.04	16.26 ± 10.22	n.s 0.41
N1	6.54 ± 1.96	6.15 ± 2.27	n.s 0.35
D2	12.52 ± 5.10	13.23 ± 6.58	n.s 0.32
N2	5.62 ± 2.06	6.04 ± 2.59	n.s 0.38
D3	8.94 ± 2.24	9.09 ± 2.93	n.s 0.58
N3	5.49 ± 2.09	5.45 ± 2.21	n.s 0.63
D4	7.15 ± 2.35	7.34 ± 2.33	n.s 0.69
N4	5.13 ± 2.43	5.30 ± 2.01	n.s 0.65

Supplemental table 6: activity of *opn4xa* -/- versus control larvae in LL

condition	wt (n=66)	*opn4xa-/-* (n=66)	p value
D1	16.56 ± 9.57	20.15 ± 12.25	n.s 0.07
N1	3.84 ± 2.99	6.22 ± 5.60	*** 0.02**
D2	16.67 ± 7.79	19.22 ± 11.49	n.s 0.26
N2	4.90 ± 3.30	5.92 ± 4.48	n.s 0.36
D3	14.27 ± 7.16	13.94 ± 7.26	n.s 0.82
N3	5.92 ± 4.09	5.63 ± 3.75	n.s 0.70